doi.org/10.36721/PJPS.2020.33.2.SUP.795-803.1

# Equilibrium, kinetics, thermodynamics and docking studies of $Cu^{2+}$ ion adsorption over ion-exchange resin and kappa carrageenan blends in blood samples

**Saad Salman[1], Sajid Asghar[1]*, Ikram Ullah Khan[1], Syed Haroon Khalid[1], Fahad Hassan Shah[2] and Mohammad Usman[3]**

[1]Department of Pharmaceutics, Government College University, Faisalabad, Pakistan
[2]Centre of Biotechnology and Microbiology, University of Peshawar, Khyber-Pakhtunkhwa, Pakistan
[3]Department of Pharmacy, The University of Lahore (Islamabad Campus), Islamabad, Pakistan

**Abstract**: Cupric ions are hazardous to human beings and their removal from the body is very necessary. The blends of IRP69H (AMBERLITE IRP-69 [$H^+$] RESIN), DC20H (DOWEX™ 20 [$H^+$] Resin), DMSCH (DOWEX™ MARATHON™ MSC [$H^+$] Resin) and Kappa Carrageenan (κ-) were utilized for the removal of ions of $Cu^{2+}$ from the blood. They were subjected to docking studies which showed that there is no significant interaction with the blood albumin. IER dose of 0.5 mg/10mL of IRP69H/κ-, DMSCH/κ-, and DC20H/κ- was essential for the $Cu^{2+}$ ion removal. At pH 5.4, optimal $Cu^{2+}$ ions adsorption efficiency was attained. The adsorption capacities of $Cu^{2+}$ were in the order of IRP69H/κ->DC20H/κ->DMSCH/κ-. While the data fitted well to Freundlich, Langmuir and Dubinin-Radushkevich. Pseudo-second order was followed for $Cu^{2+}$ adsorption for DMSCH/κ- and DC20H/κ- while the pseudo-first order was demonstrated well for IRP69H/κ-.

**Keywords**: Adsorption, isotherm, kinetics, thermodynamics, docking, kappa-carrageenan, ion-exchange resin.

## INTRODUCTION

Novel drug delivery system has a promising impact in healthcare which not only ameliorates the patient compliance but it can help to optimize the therapeutics. Broadly, the formulation of such drug deliveries are based on two basic kinds namely, chemical principles (pro-drug, drug-polymer conjugate, drug-polymer complex and ion-exchange resin (IER) which is characterized by enzymatic degradation, hydrolysis, and ion dissociation while the other kind is the physical principles (erosion, diffusion, and osmotic pump) (Asim *et al*., 2019, Rizvi and Saleh, 2018). However, a drug-resinate system using chemical principles demonstrates its inimitable characteristics and features while using IER with the drug (Shakushiro *et al*., 2018). The activity of drug-resinate complex starts when it is taken and it binds to the receptor/target site. The binding of the receptors with the drug occurs when the ions of the body fluid interact with the polymeric matrix. The rate of ion-exchange depends upon the affinity of the ions with the ionized polymer and also to the molar concentration of the corresponding ions (Balguri *et al*., 2017). The IER and Kappa Carrageenan (κ-), an algal polysaccharide are used in many dosage forms such as lipid-lowering agents: Colestipol, cholestyramine, colesevelam, and for hyperphosphatemia in sevelamer while for potassium-lowering agent: Sodium polystyrene. They are also used as taste masking agent, tablet disintegrant, gelling and stabilizing agents (Zhang *et al*., 2019). The tremendous increase in industrial activity and the pollution all around us is increasing in the air, water, and on the land. Moreover, environmental pollution has posed severe health problems. Copper ($Cu^{2+}$) is essential to all living organisms and are extensively used in different medical/diagnostic apparatuses. But the over-accumulation of this metal in the body is hazardous. Their efficient removal from the body is not only imminent but such a safe sustained release polymer, if used for scavenging this metal ion, would be a promising technology. It is well established that the most economical strategies to remove metals from wastewater are the IER (Pahlevani *et al*., 2019). Different scientists (Shen *et al*., 2017, Edebali and Pehlivan, 2016, Lee *et al*., 2017) had paid a lot of attention to the IER sorption of $Zn^{2+}$, $Pb^{2+}$, $Cr^{3+}$, $Ni^{2+}$ and $Co^{2+}$ but only in solution or wastewater. In recent years, the computational analysis had accurately established the drug-protein interactions hence helping in the prediction analysis. The contribution of in-silico studies in the field of pharmacology and medicinal chemistry is enormous for drug candidates. But their application in surface chemistry is somewhat scarce. Here in our study, we had employed docking studies before conducting the blood adsorption modeling in-order to check our samples for a possible interaction of the IER and κ- with blood protein i.e. albumin. The studies on metal removal directly from the human blood had not been extensive whereas the adsorption of metal ions such as $Hg^{2+}$, $Cu^{2+}$, $Sb^{3+}$ and $Cd^{2+}$ is quite rare. So, $Cu^{2+}$adsorption over the resin/κ-blends were studied at different concentrations, contact time, pH and temperature in human blood samples.

**Corresponding author:* e-mail: sajidasghar@gcuf.edu.pk

## MATERIALS AND METHODS

### *Docking parameters*

The 3D ligand structures of κ- [CID 11966249], Dowex [CID 16212807], Amberlite [CID 121763185] were obtained from PubChem database. The ligand structures were subjected to refinement, energy minimization, and to relax the intra-atomic bonding between the resin and κ- through PRODRG Server. The retrieval of the receptor 3D structures from protein databank (PDB) was done. These corresponding structures were further prepared for docking studies using Modrefiner. Two active potential ligand binding sites were predicted with the assistance of Metapocket 2.0 to further validate the docking results. The rigid docking algorithm (PatchDock) (Binh *et al*., 2019) was used to carry out the nature of the interaction between the resins and κ-with human serum albumin.

### *Chemicals*

All the polymers IRP69H, DC20H, DMSCH, and κ- were purchased from Sigma Aldrich (St. Louis, United States) and Lenntech (Delfgauw, Netherlands). Their framework consists of an irregular, macromolecular matrix having three-dimensional networks of hydrocarbon chains. They can be operated over a much wider pH range (0-14). The capacity of the resin is 1.7, 2.1 and 1.6meq/mL respectively. The moisture contents vary from 45-55 % by weight. The maximum temperature which they can tolerate is 80, 120 and 150$^{o}$C respectively. Their particle size varies from 420-650±50 μm and their physical form is that of the spherical beads.

### *Reagents*

The reagents such as HCl and NaOH (BDH Chemicals, Mirqab, Kuwait) were used for the adjustment of pH. Millipore-milli-Q deionized water (BDH Chemicals, Mirqab, Kuwait), with a conductivity of 18.2mW/cm$^2$ was used for the preparation of the sample solutions. Heparin (Sigma Aldrich [St. Louis, United States]) approximately, 70-150 USP units per 10-20mL of the blood sample was used for anticoagulation in each and every experiment. The copper-sulfate ($CuSO_4$) was purchased from MERCK (Kenilworth, NJ, USA). All the glassware was soaked in 0.1% Alconox solution (Fluka-Honeywell Specialty Chemicals, Seelze, Germany) for de-ionized water for 24-hour (h). To etch out the metals, the glassware was immersed in $HNO_3$. Test tubes were washed with acids. Analytical grade solvents and materials were used in all the experiments.

### *Instruments*

pH meter type Jenway-3505 (Essex, England) was used for the determination of the pH. The shaking speed of the shaker bath was measured by thermostat (DAIHAN WSB-30, USA). The $Cu^{2+}$ ion concentration was measured spectrophotometrically over Varian atomic-absorption-spectrophotometer (VAAS) [Model AA240FS, Westford MA, USA] at 580 nm.

### *Preparation of solutions and blends*

Approximately 3.93g of $CuSO_4.5H_2O$ was utilized to make a solution of one-liter. The IER resins and κ- were taken w/w by weighing 0.1/0.1g in 1mL of distilled water to make up a physical mixture. The resulting mixture was heated to remove water molecules and the dry residue was obtained. The dried blend mixture was crushed uniformly to obtain a fine powder. The working standards of $Cu^{2+}$ ions and blend were then prepared by dilution from the stock solution. 0.1mL of heparin was utilized in all the experiments to avoid coagulation. All the experiments were conducted in triplicate.

### *Determination of adsorption of $Cu^{2+}$ in human whole blood (HWB)*

*Determination of metals in HWB and Serum*

The 5cc syringes were used to take venous blood of sixteen human volunteer blood donors at Department of Pharmacy, Abasyn University, Peshawar, Pakistan. Verbal consent was taken from the adult subjects (aged 21-23). Permissions and ethical approvals were given by IRB, Abasyn University, Peshawar, and Government College University, Faisalabad. The HWB samples were subjected to centrifuge at 2000 rpm for two mins as described by (Lim *et al*., 2017). The serum was separated from the blood and allowed to dry in an oven at 37$^{o}$C. It was then analyzed for heavy metals through VAAS by already reported method (Dhawangale *et al*., 2018).

### *Determination of adsorption of $Cu^{2+}$ at different resin/κ-blend concentrations*

For the determination of the adsorption, 1mL $Cu^{2+}$ ion solution and 0.1g w/w solution (0.1g of IER resin/0.1g of κ-) in a test tube. It was then mixed with 10cc of HWB.

### *Determination of adsorption of $Cu^{2+}$ at different pH*

The 0.1g of dried physical mixture of the blend and 1mL of $CuSO_4$ solution mixed with HWB was shaken at 37$^{o}$C for 1-h. It was then filtered with the Whatman filter paper. Determination of $Cu^{2+}$ ions at different pH values was done over the filtrate obtained.

### *Measurement of contact time*

0.1g of the blend and 1mL of the $Cu^{2+}$ ions were mixed with 10cc HWB were taken in 25mL test tubes. These blends were shaken in the temperature-controlled shaker for different intervals of time.

### *Determination of adsorption of $Cu^{2+}$ at different temperatures*

A 15 mL of the conical flask contained the blend and $CuSO_4$ in HWB were shaken at 20, 25 and 37$^{o}$C on a shaker separately for samples. The shaking speed of the shaker bath thermostat model DAIHAN WSB-30 was set to 120 rpm. After 2-h equilibration time, it was then filtered with the Whatman filter paper. The filtrate was then subjected to determine $Cu^{2+}$ ions at different temperatures.

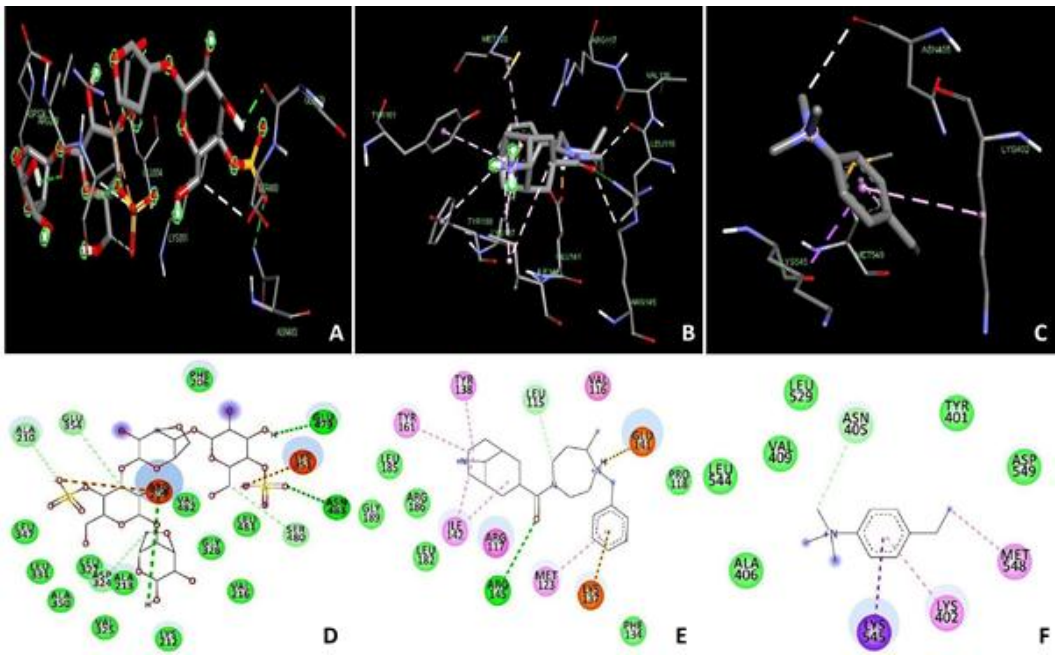


**Fig. 1**: (A) The 3D docking results of κ- with various amino acid residues. (B) The 3D docking results of Amberlite with various amino acid residues. (C) The 3D docking results of Dowex with various amino acid residues. (D) 2D Interaction visualization of κ- with various amino acid residues of serum albumin. (E) 2D Interaction visualization of Amberlite with various amino acid residues of serum albumin. (F) 2D interaction visualization of Dowex with various amino acid residues of serum albumin. Green lines show Van der Waals interaction, Red lines show Salt Bridge, orange lines show attractive charge, purple lines show pi-sigma bond, dark pink lines show ally interaction, whereas light pink color shows pi-alkyl bonds. κ- and Amberlite non-covalently interacted with active amino acid residues of human serum albumin. The H-bond length of κ- with Human Albumin amino acid residue was 2.20Å with ARG209, 2.29Å with ASN483, and 2.02Å with GLU479 whereas in case of Amberlite 4.96Å with ARG145. As shown in docking results: fig. 1D, 1E and 1F.

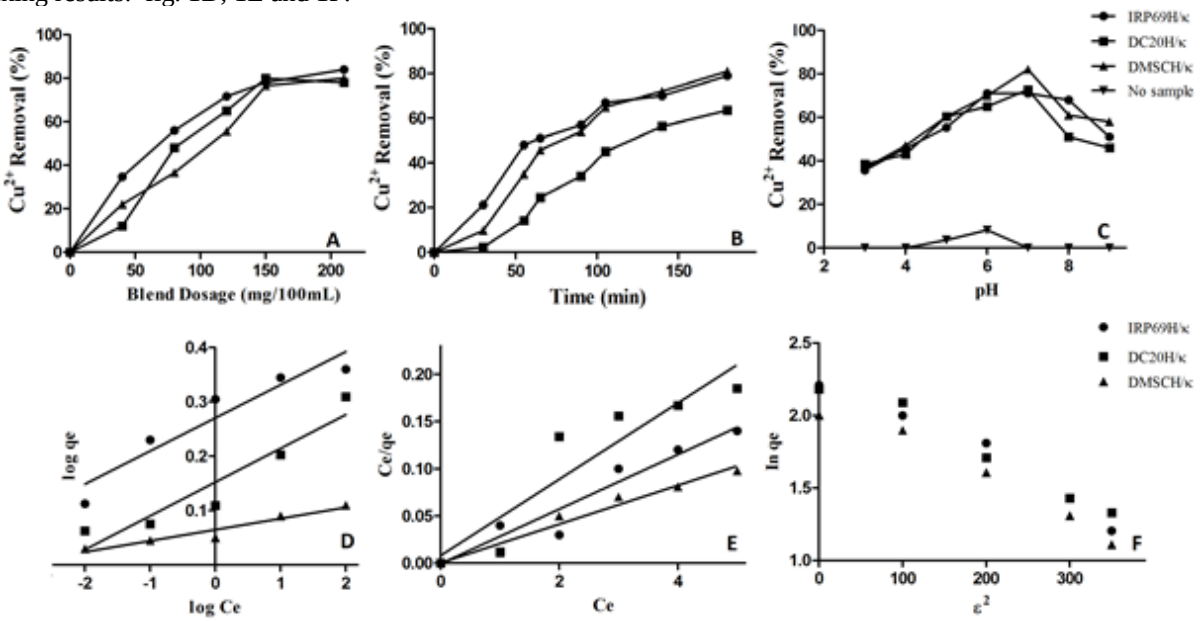


**Fig. 2**: (A) Blend dosage effect on $Cu^{2+}$ ion removal by IRP69H/κ-, DC20H/κ-, DMSCH/κ-, (B) Contact time effect on $Cu^{2+}$ ion removal, (C) pH effect on adsorption of $Cu^{2+}$, (D) Freundlich adsorption isotherm, (E) Langmuir adsorption isotherm and (F) D-R adsorption isotherm for IER: IRP69H/κ-, DC20H/κ-, and DMSCH/κ-. Each data point showed the blend dosage starting from zero to approx. 220 mg/100 mL. The blend IRP69H/κ- showed a regular and maximum adsorptive capacity of $Cu^{2+}$ followed by DC20H/κ-, and DMSCH/κ- (fig. 1A).

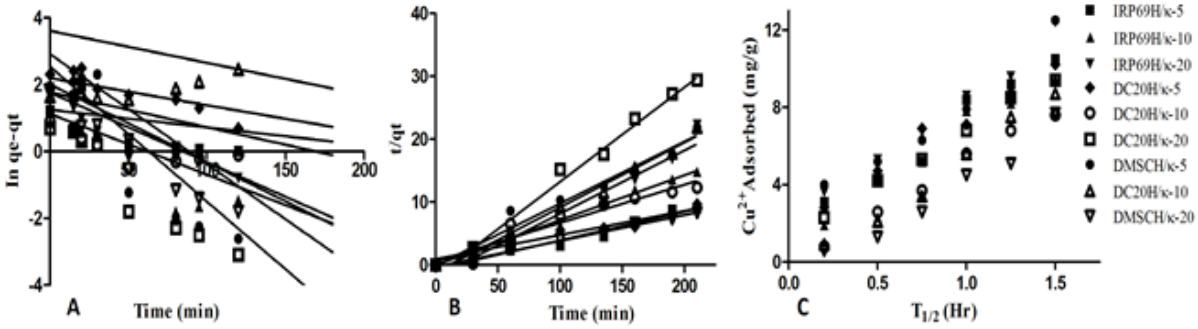


**Fig. 3**: (A) PFOK for $Cu^{2+}$ adsorption over IRP69H/κ-, DC20H/κ- and DMSCH/κ-, (B) PSOK for $Cu^{2+}$ adsorption over IRP69H/κ-, DC20H/κ-, and DMSCH/κ-,(C) $Cu^{2+}$ adsorption plot for IPDM on IRP69H/κ-, DC20H/κ- and DMSCH/κ-.

**Table 1**: Metals in serum and whole blood levels (mg/mL) of Pakistani population (N=16).

| Metals | Serum levels | | Whole blood levels | |
|---|---|---|---|---|
| | Mean | SE | Mean | SE |
| Zn | 0.1103 | 0.0985 | 0.0058 | 0.0002 |
| Fe | 0.0068 | 0.1672 | 41.067* | 1.3450 |
| Cd | 0.0043 | 0.0652 | 0.0023 | 0.9308 |
| Pb | 0.0012 | 0.0208 | 0.0045 | 0.0576 |
| Ca | 0.0005 | 0.0999 | 5.0552* | 0.1003 |
| Ni | 0.0803* | 0.0067 | 0.0955 | 0.0030 |
| Mn | 0.0682 | 0.0001 | 0.0663 | 0.0815 |
| Cr | 0.0051 | 0.0135 | 0.0012 | 0.0056 |
| Cu | 0.0056 | 0.0971 | 0.0873 | 0.0565 |

SE (Standard Error)

**Table 2**: The effect of temperature on the adsorption of $Cu^{2+}$ over the blends

| IRP69H | | DC20H | | DMSCH | | κ- | | IRP69H/κ- | | DC20H/κ- | | DMSCH/κ- | |
|---|---|---|---|---|---|---|---|---|---|---|---|---|---|
| Log Kd | T (K) | Log Kd | T (K) | Log Kd | T (K) | Log Kd | T (K) | Log Kd | T (K) | Log Kd | T (K) | Log Kd | T (K) |
| 1.6 | 290 | 0.8 | 271 | 0.5 | 248 | 0.2 | 198 | 0.9 | 176 | 1.2 | 260 | 0.7 | 241 |
| 1.8 | 297 | 1.3 | 278 | 0.9 | 260 | 0.4 | 210 | 1.8 | 185 | 1.9 | 290 | 1.2 | 264 |
| 2.1 | 315 | 1.5 | 302 | 1.3 | 289 | 0.9 | 225 | 2.2 | 201 | 2.7 | 308 | 1.5 | 282 |
| 2.2 | 325 | 2.3 | 310 | 2.3 | 311 | 1.1 | 267 | 2.6 | 218 | 2.9 | 323 | 1.8 | 300 |
| 2.5 | 348 | 3.5 | 330 | 2.6 | 322 | 1.5 | 288 | 2.9 | 238 | 3.1 | 340 | 2.0 | 312 |

**Table 3**: Computed Freundlich sorption capacity (K) and intensity of sorption (n) for $Cu^{2+}$ sorption on IER vs kappa (Concentration range 5-20 mg/L) at different pH values and at a constant temperature of 37 $^{o}$C

| Material | pH=3 | | | pH=5 | | | pH=7 | | | pH=9 | | |
|---|---|---|---|---|---|---|---|---|---|---|---|---|
| | 1/n | n | K | 1/n | n | K | 1/n | n | K | 1/n | n | K |
| IRP69H/κ | 0.47 | 2.49 | 2.28 | 0.38 | 3.03 | 4.40 | 0.30 | 2.53 | 3.45 | 0.61 | 3.5 | 2.66 |
| DC20H/κ | 0.26 | 2.74 | 2.83 | 0.28 | 4.49 | 4.62 | 0.27 | 3.46 | 4.01 | 0.12 | 3.5 | 1.38 |
| DMSCH/κ | 0.29 | 2.01 | 2.55 | 0.25 | 3.45 | 5.08 | 0.27 | 3.24 | 3.05 | 0.21 | 2.4 | 3.85 |

**Table 4**: Computed Freundlich sorption capacity (K) and intensity of sorption (n) for $Cu^{2+}$ sorption on IER vs kappa car- (Concentration range 20-50 mg/L) at different pH values and at a constant temperature of 37 $^{o}$C

| Material | pH=3 | | | pH=5 | | | pH=7 | | | pH=9 | | |
|---|---|---|---|---|---|---|---|---|---|---|---|---|
| | 1/n | n | K | 1/n | n | K | 1/n | n | K | 1/n | n | K |
| IRP69H/κ | 0.41 | 1.11 | 1.73 | 0.42 | 2.55 | 2.65 | 0.49 | 2.4 | 2.56 | 0.74 | 4.1 | 2.15 |
| DC20H/κ | 0.35 | 2.98 | 2.41 | 0.40 | 3.28 | 3.82 | 0.45 | 3.7 | 2.50 | 0.58 | 2.9 | 3.21 |
| DMSCH/κ | 0.67 | 1.49 | 1.05 | 0.33 | 3.03 | 3.47 | 0.49 | 2.54 | 2.45 | 0.61 | 3.6 | 2.45 |

**Table 5**: Computed Langmuir sorption maxima (b) and sorption energy constants (K) for $Cu^{2+}$ sorption on IER vs kappa car- (Concentration range 5-20 mg/L) at different pH values and at a constant temperature of 37°C

| $Cu^{2+}$ | pH=3 | | pH=5 | | pH=7 | | pH=9 | |
|---|---|---|---|---|---|---|---|---|
| | b(mg/g) | K(L/mg) | b(mg/g) | K(L/mg) | b(mg/g) | K(L/mg) | b(mg/g) | K(L/mg) |
| IRP69H/κ | 33.100 | 0.0302 | 45.500 | 0.0210 | 40.22 | 0.0266 | 40.003 | 0.0210 |
| DC20H/κ | 54.799 | 0.0100 | 43.318 | 0.0090 | 38.49 | 0.0123 | 35.700 | 0.0250 |
| DMSCH/ κ | 37.030 | 0.0250 | 23.409 | 0.0602 | 24.28 | 0.0254 | 27.007 | 0.0100 |

**Table 6**: Computed Langmuir sorption maxima (b) and sorption energy constants (K) for $Cu^{2+}$ sorption on IER vs kappa car- (Concentration range 20-50 mg/L) at different pH values and at a constant temperature of 37°C

| $Cu^{2+}$ | pH=3 | | pH=5 | | pH=7 | | pH=9 | |
|---|---|---|---|---|---|---|---|---|
| | b(mg/g) | K(L/mg) | b(mg/g) | K(L/mg) | b(mg/g) | K(L/mg) | b(mg/g) | K(L/mg) |
| IRP69H/κ | 17.630 | 0.0845 | 13.656 | 0.0676 | 14.44 | 0.0854 | 17.673 | 0.0845 |
| DC20H/κ | 28.543 | 0.0652 | 26.345 | 0.0835 | 27.31 | 0.0787 | 25.878 | 0.0962 |
| DMSCH/ κ | 14.030 | 0.1904 | 17.774 | 0.1904 | 16.44 | 0.1701 | 12.324 | 0.0923 |

**Table 7**: $Cu^{2+}$ isotherms for IRP69H/κ-, DC20H/κ-, and DMSCH/κ-

| Samples | Dubinin-Radushkevich, qe =qSexp -Bε$^2$ | | | Langmuir, q*e*=Q*o*bC*e*/1bC*e* | | | Freundlich, qe =$K_F Ce^n$ | | |
|---|---|---|---|---|---|---|---|---|---|
| | qs/mg g$^{-1}$ | E | $R^2$ | Qo/mg g$^{-1}$ | b/l mg$^{-1}$ | $R^2$ | $K_F$/mg g$^{-1}$ | n | $R^2$ |
| RP69H/κ- | 22.63 | 2.22k | 9.998 | 32.055 | 4.25 | 9.987 | 15.213 | 0.76 | 0.966 |
| DC20H/κ- | 18.46 | 2.15k | 9.987 | 43.565 | 1.65 | 9.966 | 12.455 | 0.67 | 0.987 |
| DMSCH/κ- | 17.73 | 2.03k | 9.983 | 38.008 | 3.25 | 9.968 | 12.076 | 0.88 | 0.976 |

**Table 8**: $Cu^{2+}$ ions metal selectivity over IER vs κ- blends.

| $Cu^{+2}$ Metal | IRP69H | DC20H | DMSCH | κ- | IRP69H/κ- | DC20H/κ- | DMSCH/κ- |
|---|---|---|---|---|---|---|---|
| Selectivity | 0.6277 | 0.5694 | 0.5500 | 0.1011 | 0.0522 | 0.0367 | 0.0267 |

**Table 9**: Pseudo first, second order, and intra-particle diffusion values at different initial $Cu^{2+}$ concentrations

| $Cu^{2+}$ | DMSCH/κ- (mg/dm$^3$) | | | DC20H/κ- (mg/dm$^3$) | | | IRP69H/κ- (mg/dm$^3$) | | |
|---|---|---|---|---|---|---|---|---|---|
| | 10 | 15 | 20 | 10 | 15 | 20 | 10 | 15 | 20 |
| [1]h(mg/g) | 3.0028 | 4.8761 | 8.0255 | 4.2760 | 6.2132 | 9.3420 | 6.5565 | 9.5568 | 13.5565 |
| [2]$K_{id}$(mg/g/hrs$^{1/2}$)($R^2$) | 5.2307 (0.9559) | 4.5066 (0.9987) | 5.5677 (0.9988) | 7.1056 (0.9678) | 8.0599 (0.9767) | 9.0350 (0.9905) | 5.6866 (0.9699) | 6.5121 (0.9888) | 8.0091 (0.9180) |
| [3]$k_1$(l/hr)($R^2$) | 0.5223 (0.9987) | 0.5655 (0.9876) | 0.6655 (0.9866) | 0.6255 (0.9807) | 0.5665 (0.9885) | 0.4368 (0.9922) | 0.5123 (0.9822) | 0.5577 (0.9866) | 0.6225 (0.9329) |
| [4]k(g/mg.min)($R^2$) | 0.0488 (0.9969) | 0.03455 (0.9665) | 0.0596 (0.9956) | 0.0122 (0.9989) | 0.0277 (0.9776) | 0.0125 (0.9669) | 0.0245 (0.9888) | 0.0255 (0.9631) | 0.0296 (0.9988) |

[1]Initial $Cu^{+2}$ adsorption rate constant, [2]Intraparticle rate constant,[3]Pseudo 1st order rate constant, [4]Pseudo 2nd order rate constant.

***Equilibrium studies***

Various isotherms Freundlich (Shah *et al*., 2018)**,** Dubinin-Radushkevich (Saruchi and Kumar, 2019), and Langmuir (Shah *et al*., 2018) were then considered for equilibrium studies. The $Cu^{2+}$ selectivity for these DC20H/κ-, IRP69H/κ- and DMSCH/κ- were calculated by selecting the maximum amount of $Cu^{2+}$ ions taken by these blends at room temperature.

***Kinetic studies***

Kinetic investigations were performed for $Cu^{2+}$. Weber Morris' intraparticle ($k_{id}$) steady rate given as $q = k_i dt^{1/2}$. The plots for DC20H/κ-, IRP69H/κ- and DMSCH/κ- of 'q' versus '$t_{1/2}$' were ascertained.

## STATISTICAL ANALYSIS

The statistical analyses such as means and standard errors of the means were calculated using IBM SPSS version 20.0.

## RESULTS

***Docking studies***

Interaction profile of three ligands named Amberlite (-232.43 kj/mol), Dowex (-136.43 kj/mol) and κ-(-231.27 kj/mol) with human albumin revealed that the resins did not show considerable interaction but the κ-did demonstrate good interaction (fig. 1A). Amberlite established one H-bond, Dowex showed no H-bonds and

with just weak van der Waals interaction as shown in fig. 1B and 1C.

***Concentration effect on the blend adsorption***

The HWB and serum samples from 16 human volunteers had different metals in their blood as shown in table 1. Different metals were detected in human blood as well as serum such as Zn, Fe, Cd, Pb, Ca, Ni, Mn, Cr and Cu. The elemental Fe was found most in the HWB with a mean of 41.067 (SE=1.3450) followed by Ca with a mean of 5.0552 (SE=0.1003). Whereas in serum, the highest levels of the metal present were Zn with a mean of 0.1103 (SE=0.0985) followed by Ni with a mean of 0.0803 (SE=0.006).

***Contact time effect on the blend adsorption***

Contact time of $Cu^{2+}$ adsorbed over the blends were found by taking 0.1/0.1 g w/w of the blends with 1 mL $CuSO_4$ solution mixed with 5cc of blood. 0.1 mL of heparin was also added to the test tube to avoid coagulation. These samples were then subjected to temperature-controlled shakers for different time intervals. It took 210 mins for the maximum adsorption of $Cu^{2+}$ over the blends. In fig. 2B, the contact time for the adsorption of $Cu^{2+}$ over the blends are shown. IRP69H/κ- showed rapid percent adsorption of $Cu^{2+}$ followed by DMSCH/κ- and DC20H/κ-.

***pH effect on the blend adsorption***

pH is the most critical aspect of the $Cu^{2+}$ adsorption that impacts the whole phenomenon. The capacity of IER to take up metal particles depends on the degree of the sulphonic groups attached as well as their interaction with the metal ions (Alguacil, 2019). Whereas, the degree of ionization, surface charge, and $Cu^{2+}$ ion speciation is effectively controlled by the pH of the solution (Espinosa *et al*., 2019). $Cu^{2+}$ adsorptions on IRP69H/κ-, DC20H/κ-, and DMSCH/κ- at different values of pH are shown in fig. 2C. The graph showed that IRP69H/κ-, DC20H/κ-, DMSCH/κ- started adsorbing $Cu^{2+}$ ions at a pH range of 3-4 but the maximum adsorption was in the range of 5.5 to 7.5 in blood.

***Temperature effect on the blend adsorption***

It was demonstrated that there is a positive effect of temperature over $Cu^{2+}$ ions adsorption over the blends. The effects of increasing the temperatures of DMSCH/κ- from 293-310 K had increased the log $K_d$ value from 0.61 to 2.7 (table 2).

***The equilibrium studies***

*Freundlich Isotherm*

The equation for Freundlich isotherm is given as (Shah *et al*., 2018):

$$qe = KCe^{\frac{1}{n}} \quad (2)$$

However, qe is the measure of $Cu^{2+}$ adsorption (mg/g), K is the adsorption constant, $Cu^{2+}$ ion Equilibrium concentration, Ce. Empirical constants are the n & K, representing the intensity and capacity of adsorption respectively. Taking eq. (2) the logarithmic form:

$$\log qe = \log K + \frac{1}{n}\log Ce \quad (3)$$

Fig. 2D demonstrate that the information for adsorption of $Cu^{2+}$ onto the blends fit well to the isotherm of Freundlich. Computed Freundlich adsorption capacity (K) and intensity of sorption (n) for $Cu^{2+}$adsorption on IER vs κ- (Concentration range 5-20 vs 25-50 mg/0.05 L) at different pH values and at a constant temperature of 37 $^oC$ has been shown in the table 3 and table 4. This table demonstrates that K values are elevated at low pH.

***Langmuir Isotherm***

The Langmuir equation for ion adsorption can be given as (Shah *et al*., 2018):

$$\frac{ce}{qe} = \frac{1}{KVm} + \frac{Ce}{Vm} \quad (4)$$

However, 'qe' is the proportion of $Cu^{2+}$sorbed per unit (mg/g), K is the adsorption constant, Equilibrium concentration, Ce and adsorption maximum as Vm. Computed Langmuir adsorption capacity (K) and intensity of adsorption (n) for $Cu^{2+}$ adsorption on IER vs κ- at different pH values and at a constant temperature of 37$^oC$ have been shown in the table 5 and table 6. Fig. 2E demonstrates the plots of Ce/qe versus Ce, exhibiting the adsorption data of $Cu^{2+}$ onto DC20H/κ, IRP69H/κ- and DMSCH/κ-. The adsorption of $Cu^{2+}$ over these blends fitted well for the Langmuir model.

***Dubinin-Radushkevich (D-R) Isotherm***

The D-R equation, an adaptation of Polanyi theory, explains a quantitative micro-porous adsorption of different sorbents. This equation helps to understand the mechanism of micropore adsorption and basically rejects the idea of layer-by-layer adsorption phenomenon of Langmuir. It facilitates the idea of pore-filling and supports only those sorbents that involves van der Waals forces. D-R isotherm can further explain the adsorptive phenomenon but rejects the homogeneity of the surface. The equation can be given as follows (Saruchi and Kumar, 2019):

$$qe = qsexp - B^{e^2} \quad (5)$$

Where the correlation of this equation gives rise to:

$$E = \frac{1}{(2B)^{\frac{1}{2}}} \quad (6)$$

The results in fig. 2F have demonstrated that all the blends have shown nearly similar adsorption energy. The summary of the isotherms is given in table 7.

***Selectivity of $Cu^{2+}$ ions***

Selectivity is the capacity of picking off one ion over another. The selectivity of different blends is shown in

table 8. The proportion of $Cu^{2+}$ adsorption selectivity relies upon the ionic structure, pH and ion-resin shape. In our study, the IRP69H/κ- had the highest capacity of 0.0522mmol/g at 37°C followed by DMSCH/κ- (0.0367mmol/g), and DC20H/κ- (0.0267mmol/g).

***The kinetic studies***

*Pseudo-First-Order Kinetics*

The equation of PFOK can be given as (Khan *et al*., 2018):

$$\frac{dqt}{dt} = k_1(qe - qt) \quad (7)$$

The first order rate constant of adsorption is shown $k_1$, qe is the adsorbed $Cu^{2+}$ amount, whereas qt is the adsorbed $Cu^{2+}$ at time interval 't'.

The following expression is obtained after the integration of the above equation:

$$\ln(qe - qt) = k_1 t + C_1 \quad (8)$$

Where $C_1$ is the first order integration constant. If suppose, q=0 at t = 0, then:

$$\ln(qe - qt) = \ln qe - k_1 t \quad (9)$$

The data sets show that the blends did not follow the pseudo-first-order kinetics very well. (fig. 3A).

***Pseudo-Second-Order Reaction Kinetics***

Adsorption kinetics was calculated by the use of the following equations (Khan *et al*., 2018):

$$\frac{dqt}{dt} = k_2(qe - qt)^2 \quad (11)$$

Where $C_2$ is the second order integration constant. Algorithmic arrangement of the equation gives the following expression:

$$\frac{t}{dt} = \frac{1}{k_2 qe^2} + \frac{t}{qe} \quad (12)$$

We had utilized the $Cu^{2+}$ as 5, 10, 20 mg/0.05 L individually. The evaluation of adsorption rate for $Cu^{2+}$ was done by utilizing first and second-order of pseudo-kinetics. The ln (qe–qt) showed nearly a straight line for all the blends. The pseudo-first and second order of $Cu^{2+}$ adsorption has been shown in fig. 3B. The calculation for $k_1$ and $k_2$ were completed by the help of slope. All the blends did show good pseudo-second-order reaction kinetics.

***Intraparticle-Diffusion Model***

Weber Morris (Kamaruddin *et al*., 2017) has given the intraparticle diffusion ($k_{id}$) model as:

$$q = k_i dt^{1/2} \quad (13)$$

Where the $k_{id}$ values for each metal ion were calculated from the slope, the amount adsorbed 'q' expressed in terms of (mg/g) at a given time interval, t (hr) (fig. 3C). $Cu^{2+}$ ion dispersion is not efficient for DC20H/κ- as compared to IRP69H/κ- and DMSCsH/κ- having high dispersion rates. At the point when a $Cu^{2+}$ particle diffuses into the cationic groups; diffusion is more but the distribution rate diminishes. The summary of all these factors are given in table 9.

## DISCUSSION

Docking study of resins and κ- with serum albumin protein had helped in conducting the adsorption studies. The ligands Amberlite and Dowex did not show considerable interaction with albumin protein. But κ- non-covalently interacted with active amino acid residues of albumin. The whole blood and serum Cu levels have shown great agreement with (Dhawangale *et al*., 2018). But relatively lower Ca and Fe levels reported in the literature (Lim *et al*., 2017). The IRP69H/κ- had the highest capacity of adsorbing $Cu^{2+}$, 0.453 mmol/g at 37 °C, followed by DMSCH/κ- (0.0922 mmol/g) and DC20H/κ- (0.0194 mmol/g). Ebdali and Pehlivan (Edebali and Pehlivan, 2016) had discussed the pH effect of 4.4 to 5.6 of $Cu^{2+}$ removal from IER. The capacity of $Cu^{2+}$ adsorption was significantly increased at the pH range of 3-5. But a further increase in pH resulted in a decrease in the adsorption capacity of the blends due to the saturation of the sites of the blends as well as the phenomenon of the surface alteration as seen by other researchers (Pagano *et al*., 2016, Sun *et al*., 2016). The absorbance acquired at a particular pH and temperature exhibited that at the span of 2-5 mins the relative retention was nearly zero and continued with the passage of time. This implies that $Cu^{2+}$ ions were not interacting with the blends in the very beginning as reported by other scientists (Demiral and Güngör, 2016, Timur and Paşa, 2018). Then after 5-10 mins the adsorption of $Cu^{2+}$ ions were enhanced because of the dynamic sites of the considerable number of active sites were not completely involved (Vhahangwele and Mugera, 2015). One of the most important and understudied parameters for the adsorption of $Cu^{2+}$ is the thermodynamic parameters (Edebali and Pehlivan, 2016). The negative impact of the temperature on $Cu^{2+}$ adsorption was seen by Wycisk and his colleagues (Wycisk *et al*., 2017), (Shen *et al*., 2017, Jia *et al*., 2017). Because of this, more steady chelating buildings are framed at elevated temperatures between di-phosphonic groups and $Cu^{2+}$ ions (Al-Senani and Al-Fawzan, 2018, Phuntsho *et al*., 2016). Unique selectivity impacts have appeared via carboxylic and phosphonic groups towards the multivalent particles. At pH 7, Chen and other colleagues (Chen *et al*., 2015, Shah *et al*., 2018, Khan *et al*., 2018) reported the following pattern of adsorption for $Mg^{2+}<Ca^{2+}<Ni^{2+}<Co^{2+}<Cu^{2+}$ for cationic-exchangers. The estimations of adsorption maxima (b) nearly takes after a similar pattern as shown in other studies (Ruder *et al*., 2019, Liu *et al*., 2019) . Langmuir is

the best model to compute capacity of adsorption of DC20H/κ-, IRP69H/κ-, and DMSCH/κ- (Edebali and Pehlivan, 2016, Pagano *et al*., 2016). One of the theories states that sulphonate groups present in these IERs effectively quench cations (Kim *et al*., 2019, Hu *et al*., 2019). While contemplating the adsorption of metal particles $Fe^{3+}$, $Cr^{2+}$, $Al^{3+}$ and $Be^{2+}$ reasoned that the metal particles which had higher electrical potential and lower pH of the hydrolysis were promptly taken by the cationic-exchangers (Phuntsho *et al*., 2016). In our study, PSOK was followed for $Cu^{2+}$ adsorption of DMSCH/κ- and DC20H/κ- while the PFOK was demonstrated well for IRP69H/κ-. In majority of the studies, the IER follows PSOK (Shah *et al*., 2018, Khan *et al*., 2018), (Phuntsho *et al*., 2016, Fulke *et al*., 2015, Brudey *et al*., 2016).

## CONCLUSIONS

IRP69H/κ-, DC20H/κ- and DMSCH/κ- demonstrated tremendous potential for adsorbing $Cu^{2+}$ ions. A dose of 0.5mg/10mL of IRP69H/κ-, DMSCH/κ- and DC20H/κ- was essential for the $Cu^{2+}$ ion removal. The $Cu^{2+}$ adsorption increased with pH, concentration, temperature, and contact time of the solution to a certain limit. At pH 5.4, optimal $Cu^{2+}$ ions adsorption efficiency was attained. The adsorption capacities of $Cu^{2+}$ were in the order of IRP69H/κ->DC20H/κ->DMSCH/κ-. The adsorption data fitted well to Freundlich, Dubinin-Radushkevich, and Langmuir. Pseudo-second order was followed for $Cu^{2+}$ adsorption for DMSCH/κ- and DC20H/κ- while the pseudo-first order was demonstrated well for IRP69H/κ-. It is suggested that further studies should be done to check the *in-vivo* $Cu^{2+}$ ions adsorption. Our research is a pilot study and we tried our best to control the conditions of the experiments, however, many factors could not be controlled. To resolve the issue regarding the coagulation of blood samples, Heparin $Na^{+}$ ion was used, whose affinity for $Cu^{2+}$ ions could have interacted with the overall adsorption. Due to the 'fear' of coagulation and denaturing of the blood samples, we could not shake the samples for longer periods of time. The blood samples contained different elements, which can lead to varying adsorption capacities. Elevation of temperatures for thermodynamic studies could have lead to hemolysis therefore; extensive studies at varying temperatures were not possible.

## REFERENCES


Abu-Saied MA, Wycisk R, Abbassy MM, El-Naim GA, El-Demerdash F, Youssef ME, Bassuony H and Pintauro PN (2017). Sulfated chitosan/PVA absorbent membrane for removal of copper and nickel ions from aqueous solutions Fabrication and sorption studies. *Carbohydr. Polym.*,**165**(11): 149-158.

Adelli GR, Balguri SP, Bhagav P, Raman V and Majumdar S (2017). Diclofenac sodium ion exchange resin complex loaded melt cast films for sustained release ocular delivery. *Drug Deliv.*, **24**(1): 370-379.

Al-Senani GM and Al-Fawzan FF (2018). Study on adsorption of Cu and Ba from aqueous solutions using nanoparticles of Origanum (OR) and Lavandula (LV). *Bioinorg. Chem. Appl.*, 2018.

Alguacil FJ (2019). The removal of toxic metals from liquid effluents by ion exchange resins. Part IX: lead (II)/H+/Amberlite IR-120. *Rev. Metal.*, **55**(1): e138.

Bezzina JP, Ruder LR, Dawson R and Ogden MD (2019). Ion exchange removal of Cu(II), Fe(II), Pb(II) and Zn(II) from acid extracted sewage sludge Resin screening in weak acid media. *Water Res.*, **158**(13): 257-267.

Chandra S, Dhawangale A and Mukherji S (2018). Hand-held optical sensor using denatured antibody coated electro-active polymer for ultra-trace detection of copper in blood serum and environmental samples. *Biosens. Bioelectron.*, **110**: 38-43.

Chang Y, Shen C, Li P-Y, Fang L, Tong Z-Z, Min M and Xiong C-H (2017). Optimization of polyacrylonitrile–cysteine resin synthesis and its selective removal of Cu(II) in aqueous solutions. *Chinese Chem. Lett.*, **28**(2): 319-323.

Chekli L, Phuntsho S, Kim JE, Kim J, Choi JY, Choi J-S, Kim S, Kim JH, Hong S, Sohn J and Shon HK (2016). A comprehensive review of hybrid forward osmosis systems: Performance, applications and future prospects. *J. Mem. Sci.*, **497**(1): 430-449.

Cobbina SJ, Chen Y, Zhou Z, Wu X, Zhao T, Zhang Z, Feng W, Wang W, Li Q, Wu X and Yang L (2015). Toxicity assessment due to sub-chronic exposure to individual and mixtures of four toxic heavy metals. *J. Hazad. Mater.*, **294**(16): 109-120.

Demiral H and Gungor C (2016). Adsorption of copper(II) from aqueous solutions on activated carbon prepared from grape bagasse. *J. Clean. Prod.*, **124**(12): 103-113.

Edebali S and Pehlivan E (2016). Evaluation of chelate and cation exchange resins to remove copper ions. *Powder Tech.*, **301**(15): 520-525.

Giripunje MD, Fulke AB and Meshram PU (2015). Remediation techniques for heavy-metals contamination in lakes: A mini-review. *Clean-Soil, Air, Water.*, **43**(9): 1350-1354.

Guo Y, Jia Z and Cao M (2017). Surface modification of graphene oxide by pyridine derivatives for copper (II) adsorption from aqueous solutions. *J. Ind. Eng. Chem.*, **53**(18): 325-332.

Han X, Zhang S, Chai Z, Dong Y, He W, Yin L, Yang L and Qin C (2019). *In vitro* and *in vivo* evaluation of the taste-masking efficiency of Amberlite IRP88 as drug carries in chewable tablets. *J. Drug Deliv. Sci. Tec.*, **49**(1): 547-555.

Javed R, Shah LA, Sayed M and Khan MS (2018). Uptake of heavy metal ions from aqueous media by hydrogels and their conversion to nanoparticles for

generation of a catalyst system: two-fold application study. *RSC Advances.,* **8**(27): 14787-14797.

Junior ABB, Espinosa DCR, Dreisinger D and Tenório JAS (2019). Effect of PH to recover Cu (II), Ni (II) and Co (II) from nickel laterite leach using chelating resins. *Tecnol. Metal Mater. Min.,* **16**(1): 135-140.

Kim HJ, Lim HS, Lee KR, Choi MH, Kang NM, Lee CH, Oh EJ and Park HK (2017). Determination of Trace Metal Levels in the General Population of Korea. *Int. J. Environ. Res. Public Health*, **14**(7): 702-702.

Largitte L, Brudey T, Tant T, Dumesnil PC and Lodewyckx P (2016). Comparison of the adsorption of lead by activated carbons from three lignocellulosic precursors. *Microporous Mesoporous Mater.,* **219**(1): 265-275.

Lee CG, Lee S, Park JA, Park C, Lee SJ, Kim SB, An B, Yun ST, Lee SH and Choi JW (2017). Removal of copper, nickel and chromium mixtures from metal plating wastewater by adsorption with modified carbon foam. *Chemosphere.,* **166**(1): 203-211.

Lim WR, Kim SW, Lee CH, Choi EK, Oh MH, Seo SN, Park HJ and Hamm SY (2019). Performance of composite mineral adsorbents for removing Cu, Cd, and Pb ions from polluted water. *Sci. Rep.*, **9**(1): 13598.

Nazir I, Asim MH, Dizdarevic A and Bernkop-Schnurch A (2019). Self-emulsifying drug delivery systems: Impact of stability of hydrophobic ion pairs on drug release. *Int. J. Pharm.,* **561**(8): 197-205.

Nekouei RK, Pahlevani F, Assefi M, Maroufi S and Sahajwalla V (2019). Selective isolation of heavy metals from spent electronic waste solution by macroporous ion-exchange resins. *J. Hazard. Mater.,* **371**(11): 389-396.

Qi X, Liu R, Chen M, Li Z, Qin T, Qian Y, Zhao S, Liu M, Zeng Q and Shen J (2019). Removal of copper ions from water using polysaccharide-constructed hydrogels. *Carbohydr. Polym.,* **209**(7): 101-110.

Quan PM, Binh VN, Ngan VT, Trung NT and Anh NQ (2019). Molecular docking studies of Vinca alkaloid derivatives on Tubulin. *Vietnam J. Chem.,* **57**(6): 702-706.

Rizvi SAA and Saleh AM (2018). Applications of nanoparticle systems in drug delivery technology. *Saudi Pharm. J.,* **26**(1): 64-70.

Saruchi and Kumar V (2019). Adsorption kinetics and isotherms for the removal of rhodamine B dye and $Pb^{+2}$ ions from aqueous solutions by a hybrid ion-exchanger. *Arab. J. Chem.,* **12**(3): 316-329.

Shah LA, Khan M, Javed R, Sayed M, Khan MS, Khan A and Ullah M (2018). Superabsorbent polymer hydrogels with good thermal and mechanical properties for removal of selected heavy metal ions. *J. Clean. Prod.,* **201**(21): 78-87.

Timur M and Pasa A (2018). Synthesis, Characterization, Swelling and Metal Uptake Studies of Aryl Cross-Linked Chitosan Hydrogels. *ACS Omega.,* **3**(12): 17416-17424.

Vhahangwele M and Mugera GW (2015). The potential of ball-milled South African bentonite clay for attenuation of heavy metals from acidic wastewaters: Simultaneous sorption of $Co^{2+}$, $Cu^{2+}$, $Ni^{2+}$, $Pb^{2+}$, and $Zn^{2+}$ ions. *J. Environ. Chem. Eng.,* **3**(4 A): 2416-2425.

Volpe A, Pagano M, Pastore C, Cuocci C and Milella A (2016). Sorption properties of an amorphous hydroxo titanate towards $Pb^{2+}$, $Ni^{2+}$ and $Cu^{2+}$ ions in aqueous solution. *J. Environ. Sci. Heal. A.,* **51**(13): 1121-1130.

Wang YH, Hu HP and Qiu XJ (2019). Fixed-bed column study for deep removal of copper (II) from simulated cobalt electrolyte using polystyrene-supported 2-aminomethylpyridine chelating resin. *J. Cent South Univ T.,* **26**(5): 1374-1384.

Yang F, Sun S, Chen X, Chang Y, Zha F and Lei Z (2016). Mg–Al layered double hydroxides modified clay adsorbents for efficient removal of $Pb^{2+}$, $Cu^{2+}$ and $Ni^{2+}$ from water. *Appl. Clay Sci.,* **123**(5): 134-140.

Yoshida T, Shakushiro K and Sako K (2018). Ion-responsive drug delivery systems. *Curr. Drug Targets.,* **19**(3): 225-238.

Zamri MFMA, Kamaruddin MA, Yusoff MS, Aziz HA and Foo KY (2017). Semi-aerobic stabilized landfill leachate treatment by ion exchange resin: Isotherm and kinetic study. *Appl. Water Sci.,* **7**(2): 581-590.